

# Model-based assessment of the role of human-induced climate change in the 2005 Caribbean coral bleaching event

Simon D. Donner<sup>\*†</sup>, Thomas R. Knutson<sup>‡</sup>, and Michael Oppenheimer<sup>\*§</sup>

<sup>\*</sup>Woodrow Wilson School of Public and International Affairs, Princeton University, 405a Robertson Hall, Princeton, NJ 08544; <sup>‡</sup>Geophysical Fluid Dynamics Laboratory, National Oceanic and Atmospheric Administration, P.O. Box 308, Princeton, NJ 08542; and <sup>§</sup>Department of Geosciences, Princeton University, 129 Guyot Hall, Princeton, NJ 08544

Edited by David M. Karl, University of Hawaii, Honolulu, HI, and approved January 16, 2007 (received for review November 14, 2006)

Episodes of mass coral bleaching around the world in recent decades have been attributed to periods of anomalously warm ocean temperatures. In 2005, the sea surface temperature (SST) anomaly in the tropical North Atlantic that may have contributed to the strong hurricane season caused widespread coral bleaching in the Eastern Caribbean. Here, we use two global climate models to evaluate the contribution of natural climate variability and anthropogenic forcing to the thermal stress that caused the 2005 coral bleaching event. Historical temperature data and simulations for the 1870–2000 period show that the observed warming in the region is unlikely to be due to unforced climate variability alone. Simulation of background climate variability suggests that anthropogenic warming may have increased the probability of occurrence of significant thermal stress events for corals in this region by an order of magnitude. Under scenarios of future greenhouse gas emissions, mass coral bleaching in the Eastern Caribbean may become a biannual event in 20–30 years. However, if corals and their symbionts can adapt by 1–1.5°C, such mass bleaching events may not begin to recur at potentially harmful intervals until the latter half of the century. The delay could enable more time to alter the path of greenhouse gas emissions, although long-term “committed warming” even after stabilization of atmospheric CO<sub>2</sub> levels may still represent an additional long-term threat to corals.

climate models | coral reefs | ocean warming | adaptation | symbiosis

Warm ocean temperatures can cause coral bleaching, the loss of color from reef-building corals because of a breakdown of the symbiosis with the dinoflagellate *Symbiodinium* (1). In late 2005, the anomalously warm sea surface temperatures (SST) in the Eastern Caribbean and tropical Atlantic caused mass coral bleaching across the region. Satellite observations noted levels of thermal stress far in excess of the standard bleaching thresholds, the highest in the 21-year satellite record (Fig. 1 *a* and *b*). Coral cover surveys detected bleaching of 90% of coral cover in the British Virgin Islands, 80% in the U.S. Virgin Islands, 66% in Trinidad and Tobago, 52% in the French West Indies, and 85% in the Netherlands Antilles (data available at <http://coralreefwatch.noaa.gov/caribbean2005>).

Occurrences of mass coral bleaching, like the 2005 Caribbean event, over the past 25 years have been attributed to rising ocean temperatures (2–4). Anthropogenic climate change is expected to increase the frequency and severity of coral bleaching events and threaten the health of coral reef ecosystems worldwide (3, 5, 6). Recent research on tropical Atlantic SSTs has suggested that anthropogenic forcing likely played a discernible role in the observed pronounced warming of the tropical North Atlantic since the 1970s (7–10).

In this study, we used the Geophysical Fluid Dynamics Laboratory (GFDL) climate models CM2.0 and CM2.1 to evaluate the role of anthropogenic climate forcing in the 2005 Caribbean bleaching event and the probability of events like 2005 occurring in the future. Although no individual event can be determinis-

tically attributed to human-induced climate warming, the climate model simulations enabled us to investigate the probability of an event occurring under different scenarios. First, we examined whether anthropogenic forcing played a role in ocean warming over the past 130 years in the region of the 2005 bleaching event, using replicate historical model runs and historical observations. Second, we used model simulations of background or internal climate variability to examine the probability of the 2005 thermal stress event occurring with and without past changes in radiative forcing (natural or anthropogenic). Finally, we evaluated the likelihood of similar events occurring under future climate scenarios, with or without thermal adaptation by corals and their symbionts.

## Results

We focused on the region from 75°W to 45°W, 20°N to 10°N where the maximum thermal stress was observed (via satellite) in 2005. This region encompasses corals reefs throughout the Eastern Caribbean and Lesser Antilles and also a large expanse of Atlantic Ocean with no islands; including only the western area where coral bleaching was observed in 2005 would eliminate the larger structure of the thermal anomaly. The bleaching region overlaps the “Main Development Region” for tropical Atlantic cyclones that has been the focus of recent climate studies. Main development region definitions vary slightly among existing studies (7, 8, 11).

**Predicting Coral Bleaching from SSTs.** Coral bleaching is commonly observed when the SSTs exceed the maximum monthly mean (the climatological mean temperature during the warmest month of the year) by 1°C or more for 1 month or more. The National Oceanic and Atmospheric Administration (NOAA) Coral Reef Watch program uses satellite-derived SSTs, from the Advanced Very High Resolution Radiometer (AVHRR) Pathfinder, to predict coral bleaching in real-time (12, 13). The accumulation of “degree heating weeks” (DHW) (1 week of SSTs greater than the maximum in the monthly climatology) over a rolling 12-week period serves as an effective indicator of the likelihood of bleaching (12, 13). Independent coral bleaching reports have consistently indicated that coral bleaching may begin to occur

Author contributions: S.D.D. and M.O. designed research; S.D.D. and T.R.K. performed research; S.D.D. analyzed data; and S.D.D., T.R.K., and M.O. wrote the paper.

The authors declare no conflict of interest.

This article is a PNAS Direct Submission.

Abbreviations: SST, sea surface temperature; AVHRR, Advanced Very High Resolution Radiometer; GCM, Global Climate Models; DHW, degree heating week; DHM, degree heating month; SRES, Special Report on Emissions Scenarios; AMO, Atlantic Multidecadal Oscillation; HadISST, Hadley Centre (U.K. Met. Office) globally complete sea-ice and sea-surface temperature data set.

See Commentary page 5259.

<sup>†</sup>To whom correspondence should be addressed. E-mail: [sddonner@princeton.edu](mailto:sddonner@princeton.edu).

© 2007 by The National Academy of Sciences of the USA

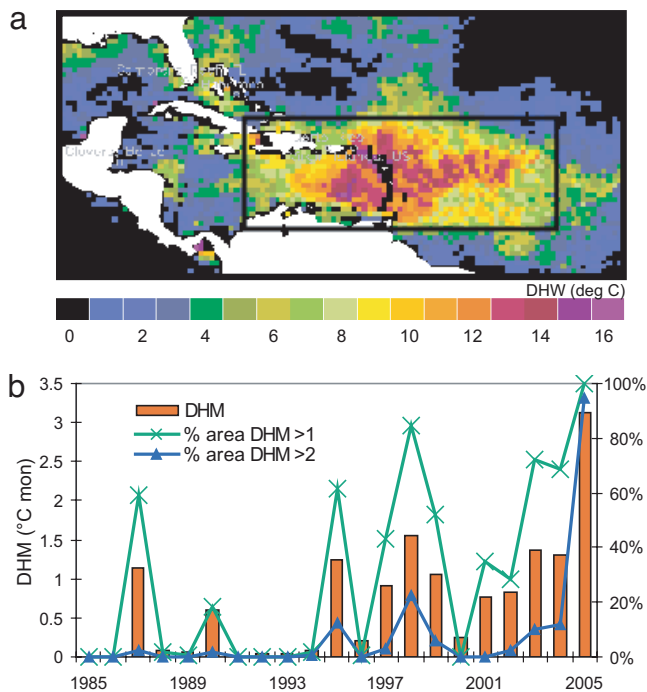


**Fig. 1.** Satellite-observed thermal stress on Eastern Caribbean coral reefs. (a) Map of 2005 maximum thermal stress, expressed as degree heating weeks ( $^{\circ}\text{C}\cdot\text{week}$ ). The study region is marked by the black line. (b) Maximum annual thermal stress during the 1985–2005 period over the study region, reinterpreted as degree heating months ( $^{\circ}\text{C}\cdot\text{month}$ ).

when the DHW is  $>4$ , and severe bleaching with some coral mortality may begin to occur when the DHW is  $>8$  (13). Although UV penetration is also critical to the occurrence of bleaching, the temperature-based prediction index is ideal for application to climate model studies (3, 5, 6).

We used the 1985–2005 AVHRR SST and DHW data (henceforth referred to as the “satellite” data) to develop a monthly bleaching prediction index more compatible with the monthly-averaged Global Climate Models (GCM) output [see Donner *et al.* (6)]. Similar to a DHW, a degree heating month (DHM; expressed as  $^{\circ}\text{C}\cdot\text{month}$ ) is equal to 1 month of SST that is  $1^{\circ}\text{C}$  greater than the maximum in the monthly climatology for that grid cell (e.g., the warmest month of the year, September or October for most grid cells in the Eastern Caribbean). Here, the DHM value was calculated over a rolling 4-month window by using the 1985–2000 period as the climatology for calculating the maximum monthly mean. There was a highly significant relationship ( $r = 0.96$ ,  $P < 0.01$ ) between the annual maximum DHM and annual maximum DHW for the study region over the 21-year record. In 2005, the maximum DHM averaged over the study region was  $3.12^{\circ}\text{C}\cdot\text{month}$ , roughly double the 1998 value, the previous high in the satellite record (Fig. 1b). A DHM value of  $2^{\circ}\text{C}\cdot\text{month}$  is roughly equivalent to the upper bleaching threshold used by the Coral Reef Watch Program (6).

**Model Simulations.** Simulated SSTs from 1870–2100 were obtained from simulations of the two new Geophysical Fluid Dynamics Laboratory global climate models: CM2.0 and CM2.1 (14). The models and forcings are described briefly in *Materials and Methods*. Model results were taken from the available “all-forcing” runs (CM2.0:  $n = 3$ ; CM2.1:  $n = 5$ ) and “natural-only” runs (CM2.0:  $n = 1$ ; CM2.1:  $n = 3$ ), where  $n$  is the number of replicate model runs conducted with different initial conditions. We averaged simulated SSTs from the individual all-

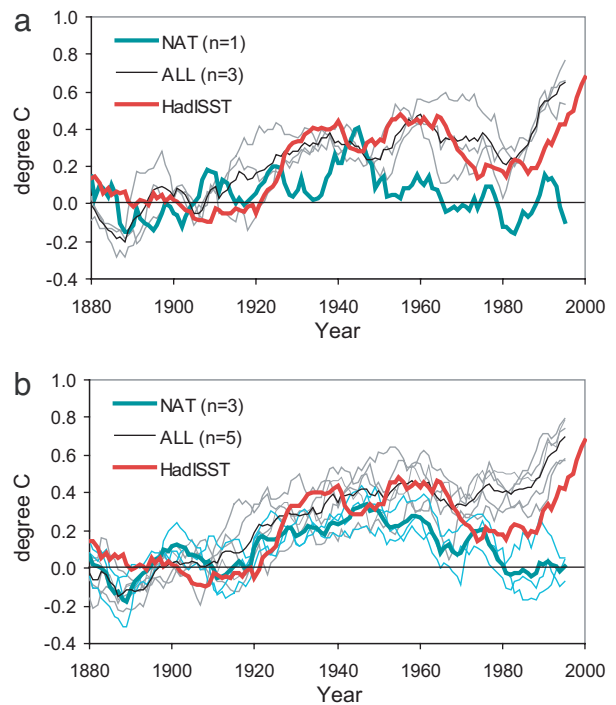


**Fig. 2.** Simulated and observed 10-year running mean SST anomalies for the period 1880–2000 in CM2.0 (a) and CM2.1 (b). The HadISST anomalies, based on data through 2005, are shown in red. The natural-only ensemble (NAT) is shown in blue, and the all-forcing ensemble (ALL) is shown in black. Individual ensemble members are shown as thin lines. The anomalies were calculated by using the 1881–1920 period as a reference period for both observations and models.

forcing (ALL) and natural-only (NAT) model runs to generate model “ensemble” results. The ensemble results from 1871–2000 were contrasted with historical SSTs from the  $1^{\circ} \times 1^{\circ}$  1870–2005 Hadley Centre (U.K. Met. Office) globally complete sea-ice and sea-surface temperature data set (HadISST; ref. 15 and <http://badc.nerc.ac.uk/data/hadisst/>) for the same period. The HadISST data set is a blend of observed SST and reconstructed SST values where observations are missing (15). It has been found to resemble other temperature reconstructions in the Caribbean region (16).

Two additional sets of model runs were used to examine background climate variability and future climate scenarios. First, the results of preindustrial “control” simulations, in which a model is run for several centuries with no changes in external forcings [CM2.0,  $t = 500$  years; CM2.1,  $t = 2,000$  years; see Delworth *et al.* (14)], were used to represent the internal climate variability in the models. Internal model drift, as measured by these control runs, is minor ( $<0.1^{\circ}\text{C}$  per century) in the subregion considered in this study. Second, two different emissions scenarios were used to contrast possible futures. The Special Report on Emissions Scenarios (SRES) A1b scenario from 2001–2100 is a representation of business-as-usual greenhouse gas emissions over this century. A second scenario from 2001–2200, based on the SRES B1 emissions path, is a representation of the effect of stabilizing atmospheric  $\text{CO}_2$  concentration at 550 ppm in the year 2100.

**Historical Trend in SSTs and DHMs.** In a previous analysis, the observed warming of the 20th century, globally and in many regions of the world, was found to be simulated more realistically in the all-forcing runs than the natural-only runs of both CM2.0 and CM2.1 (9). In the region of the 2005 hot spot, the all-forcing

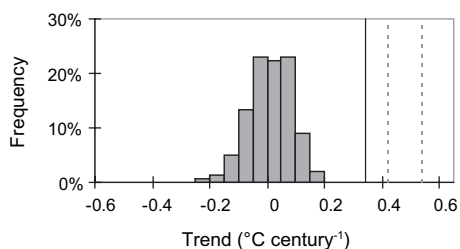


**Fig. 3.** Frequency distribution of trends ( $^{\circ}\text{C}$  per century) in 130-year segments of the control runs in CM2.0 and CM2.1 ( $n = 2,240$ ). The solid line marks the 1870–2000 trend in the HadISST data ( $0.34^{\circ}\text{C}$  per century); the dashed lines mark the 1870–2000 trend in the all-forcing ensemble mean for CM2.0 ( $0.42^{\circ}\text{C}$  per century) and CM2.1 ( $0.54^{\circ}\text{C}$  per century).

runs also generally represent the HadISST trend in annual average and August–September–October (ASO) SSTs since 1870 more realistically than the natural-only runs (Fig. 2 *a* and *b*). In CM2.0 and CM2.1, the all-forcing and natural-only SSTs both closely follow the trend in the HadISST data until the 1950s. The natural-only SSTs then diverge after the 1950s and do not represent the warming in the HadISST data since the 1970s. The anthropogenic warming signal in the models appears strong after the 1970s and is in fairly good agreement with the observed late 20th century warming, as noted in other studies (9).

The agreement between the all-forcing runs and the observations is apparent in contrasting the trends from 1870–2000 in the HadISST time series with the all-forcing ensembles, the natural-only ensembles, and the model control runs (with no forcing changes). The 130-year linear trends in ASO SSTs in the all-forcing ensemble of CM2.0 ( $0.42^{\circ}\text{C}$  per century) and CM2.1 ( $0.54^{\circ}\text{C}$  per century) are higher but on the same order as the trend in the HadISST data ( $0.34^{\circ}\text{C}$  per century). It is worth noting that the HadISST trend increases to  $0.38^{\circ}\text{C}$  per century if the analysis is continued through 2004, and to  $0.39^{\circ}\text{C}$  per century through 2005, the warmest year in the time series. Conversely, there is no positive trend in the natural-only CM2.0 simulation and a slight positive trend of  $<0.04^{\circ}\text{C}$  per century in the CM2.1 natural-only ensemble. The all-forcing ensemble and HadISST trends are larger than that of any 130-year segment of the CM2.0 and CM2.1 control runs (Fig. 3). The 95th percentile trend in the control runs is  $0.14^{\circ}\text{C}$  per century, less than half the HadISST 1870–2000 trend.

It is important to evaluate whether the models are realistically simulating the internal variability in the climate system, to test whether the observed trend could be a result of unforced climate variability. The effect of the Atlantic Multidecadal Oscillation (AMO), a 60- to 80-year oscillation in North Atlantic SSTs (17, 18), on the observed SST trends, SST variability in the tropical Atlantic, and hurricane development has been a matter of debate (7, 10, 11). Our study region partially overlaps the main development regions for tropical cyclones cited in previous studies and may share some variability aspects with the AMO (18).

Adopting a technique similar to ref. 19, we estimated the magnitude of unforced climate variability by computing the power spectrum of the HadISST “unforced” time series. This is the HadISST time series with the variations due to changes in radiative forcing over time removed, represented here by subtracting the all-forcing multimodel ensemble SST from the original HadISST time series. We contrasted the variance spectra of the unforced HadISST time series with 5th to 95th percentile range of power spectra from 130-year blocks of the model control runs. The “unforced” HadISST spectrum falls within the 5th to 95th percentile range for the control run spectra at all frequencies (Fig. 4). This spectral analysis suggests that there is no statistically significant difference between the low-

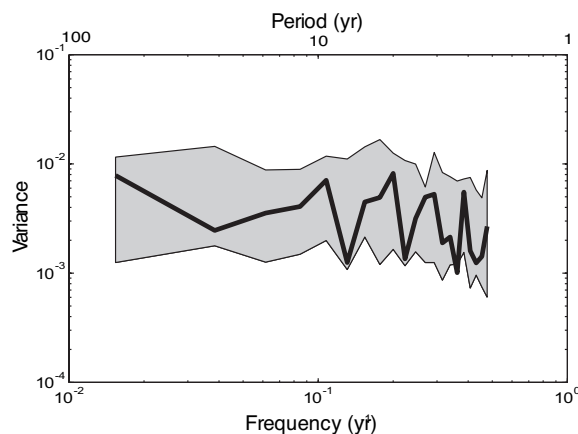


**Fig. 4.** Power spectra of observed and modeled SST over the study region. The solid line is the spectrum of the 130-year HadISST unforced residual time series, determined by subtracting the all-forcing ensemble mean from the HadISST time series. The gray region represents the 5th to 95th percentile range of power spectra computed from nonoverlapping 130-year segments of the model control runs. Linear trends were removed from the residual HadISST time series and from each of the control run time series before computing the spectra.

frequency internal variability in the models’ climate and the actual climate.

The observed low-frequency variability (centered at the 65-year period) in the spectra is at the high end of the 5th to 95th percentile range from the model control runs (Fig. 4). The magnitude of the observed variability at that frequency, expressed as the root of the variance from the spectral analysis, is 29% greater than the mean from the control run spectra. If the magnitude of the variability in the control run time series is artificially increased by 29%, the 130-year linear trends in the control runs (Fig. 3) are only marginally affected. The 95th percentile trend in the control runs increases to  $0.18^{\circ}\text{C}$  per century, roughly half the observed trend. Through a sensitivity test in which we multiplied the anomaly time series from the control runs by a series of factors, we found that the magnitude of the model’s variability, including the low-frequency variability, would have to be increased by at least 140% for the observed trend to fall within the 5th to 95th percentile range of the control runs trends. Therefore, any underrepresentation of AMO-related or other low-frequency internal variability in this region in the models would have to be dramatic to affect our conclusion that the observed warming trend is unlikely to be a manifestation of unforced climate variability alone. From these analyses, we can conclude that an anthropogenically forced warming signal is likely to be emerging from the background of natural variability in this region.

The simulations also provide insight into the historical variability in thermal stress on Eastern Caribbean reefs (Fig. 5). A previous analysis of the HadISST data and other historical SST reconstructions concluded that thermal stress may have exceeded coral bleaching thresholds (e.g., DHM  $>1$ ) in parts of the Caribbean during the 1950s and 1960s, although no observational evidence exists to confirm whether any coral bleaching occurred (16). In the HadISST data, the decadal mean DHM value averaged over the entire region of the 2005 hot spot does peak in the 1950s and 1960s, and again in the 1990s and the current decade. The DHM values for the first half of the current decade have been so high (2000–2005 mean of  $0.79^{\circ}\text{C}\text{-month}$ ) that even if there is no accumulation of thermal stress for the remainder of this decade the decadal mean DHM will still be the highest in the observed record. To test for differences between the decadal mean DHM in the model simulations runs and the

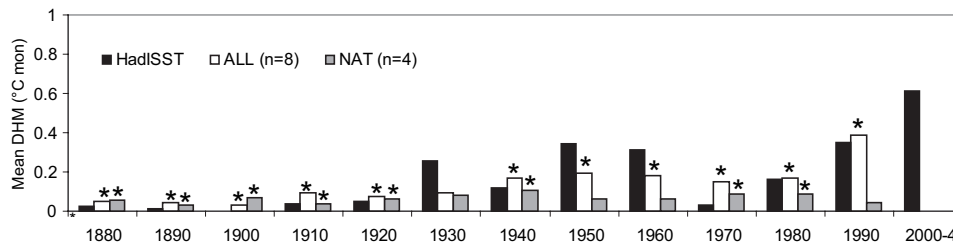


**Fig. 5.** Decadal mean DHM for the study region from 1880–2000. The model results are averaged as multimodel ensembles. The asterisks indicate no statistically significant difference between the model ensemble mean (all-forcing, or natural-only) and the HadISST data, based on a modified two-sample *t* test in which the observed data ( $n_1 = 1$ ) is assumed to have the same variance as the individual ensemble members ( $n_2 = 8$ ). The HadISST data for 2000–2004 is also shown for comparison to previous decades.

HadISST data, we performed modified two-sample *t* tests in which the HadISST data ( $n_1 = 1$ ) is assumed to have the same variance as the multi-model ensemble ( $n_2 = 8$  for the all-forcing runs;  $n_2 = 4$  for the natural-only runs). The tests found that the HadISST decadal mean DHM was significantly different from the all-forcing results only for the 1930s but was significantly different from the natural-only results for the 1930s, 1950s, 1960s, and 1990s (Fig. 5). The statistical comparison further indicates that anthropogenic forcing may have contributed to enhancing thermal stress during parts of the latter half of the 20th century.

**Probability of Occurrence.** The 1861–2000 model simulations and observed SST data sets suggest there is little historical precedent for the 2005 event. The maximum DHM averaged over the study region ( $3.12^\circ\text{C}\cdot\text{month}$ ) in the 2005 AVHRR satellite data and the fraction of the study region with  $\text{DHM} > 2^\circ\text{C}\cdot\text{month}$  (94%) were the highest both in the satellite record and in all of the CM2.0 and CM2.1 model simulations, including those with anthropogenic forcing. The 2005 maximum DHM in the HadISST data set ( $1.71^\circ\text{C}\cdot\text{month}$ ), although lower than that in the AVHRR satellite data (a difference of  $<0.5^\circ\text{C}$  per month), is still the highest in the 136-year data set. The HadISST thermal stress level for 2005 is surpassed during 0.5% of the time or 5 years in the eight all-forcing runs of CM2.0 and CM2.1 (all since the 1960s), but not once in the four natural-only runs of the two models.

We further investigated the probability of the 2005 hot spot occurring with and without anthropogenic forcing by analyzing output from control runs of the models. The preindustrial control runs of CM2.0 ( $n = 500$  years) and CM2.1 ( $n = 2,000$

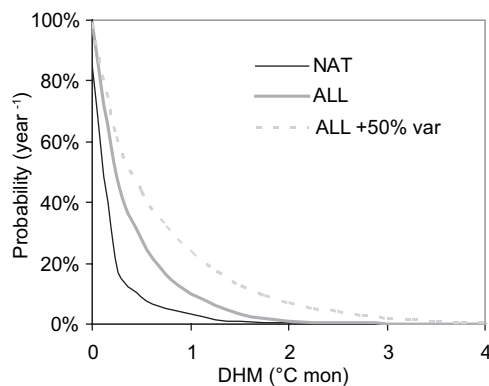


**Fig. 6.** Annual probability of DHM exceeding a threshold for the 1990s climate. As described in *Results*, a 2,500-year sample of DHMs was determined by imposing the SST anomalies from the control runs on the 1990s mean for the natural-only (NAT, in black) and all-forcing (ALL, in gray) simulations ( $n = 2,500$  years). A third simulation is shown in which the magnitude of variability in the control runs was increased by 50%.

years) represent the internal variability in the model's climate. We combined the variability in preindustrial control runs with the 1991–2000 monthly mean SSTs from the natural-only runs and again with 1991–2000 monthly mean SSTs from the all-forcing runs to generate two long-time series for analysis. Monthly anomalies in the control runs (e.g., the difference between monthly SST in January and the control run climatology for January) were estimated in 100-year intervals, to eliminate the small model drift and allow for subsampling of results. The resulting time series were used to determine probability distributions of maximum annual DHM for the study region in the present climate with and without anthropogenic forcing, similar to Stott *et al.* (19). The sampling uncertainty is estimated from the standard deviation of probabilities of the 100-year segments.

The results indicate that the thermal stress reaching the 2005 level, or a fraction of that level, would be an extremely rare occurrence without any anthropogenic forcing (Fig. 6). There is only one occurrence ( $P = 0.05\%$ ) of DHM exceeding  $1.71^\circ\text{C}\cdot\text{month}$ , the level for 2005 in the HadISST data, in the 2500-year natural-only analysis (Table 1). With anthropogenic forcing, the DHM exceeds the HadISST 2005 level in only  $2.2 \pm 1.3\%$  of the years and the satellite 2005 level in only 0.2% of the years. This result suggests that, even with the anthropogenic warming, the 2005 thermal stress is approximately a 50-year event using the HadISST data and a 500-year event using the AVHRR satellite data.

Applying the variability from the preindustrial control runs of the models implicitly assumes that there is no change in the magnitude of interannual variability in SSTs between the preindustrial and modern climate and that the model adequately simulates internal climate variability. The effect of either an underrepresentation of low-frequency variability by the models or an increase in interannual climate variability since preindustrial times was tested with a series of experiments assuming relative 1–50% increases in the interannual SST anomalies. These tests showed that, if the magnitude of the interannual SST variability is increased by 50%, the 2005 thermal stress would be a 10-year (HadISST) to 70-year (satellite) event using the all-forcing scenarios (Fig. 6).

**Table 1. Annual probability of DHM for region exceeding threshold**

Simulation*	Probability of occurrence, %			
	DHM $\geq 3.1$	DHM $\geq 2.0$	DHM $\geq 1.7$	DHM $\geq 0.5$
NAT	0	0	<0.1	$1.3 \pm 1.3$
ALL	$0.2 \pm 0.4$	$1.1 \pm 1.1$	$2.2 \pm 1.3$	$28.3 \pm 4.7$
ALL + var <sup>†</sup>	$1.5 \pm 1.3$	$7.3 \pm 2.2$	$10.1 \pm 2.1$	$43.6 \pm 4.8$

\*As described in *Results*, the SST anomalies from the control run added to the 1990s mean for the natural-only (NAT) and all-forcing (ALL) simulations.

<sup>†</sup>The magnitude of the variability in the control runs is increased by 50%.

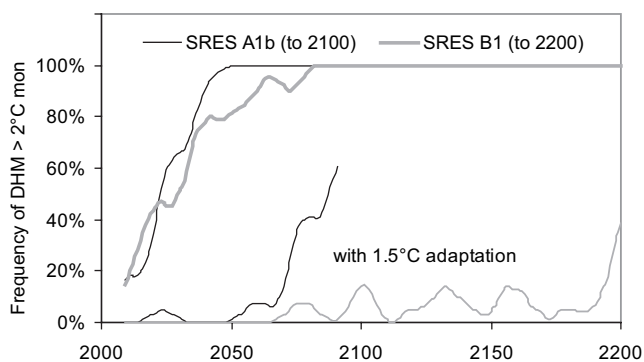


**Fig. 7.** Frequency of maximum annual DHM exceeding 2°C-month under the SRES A1b (2001–2100) and SRES B1 (2001–2200) scenarios. Shown is the ensemble decadal mean of the exceedence probability calculated for running 10-year intervals from the CM2.0 and CM2.1 simulations, assuming no thermal adaptation (thick lines) and 1.5°C thermal adaptation (thin lines).

Because the 2005 event is unprecedented in the historical data and the natural-only control simulations, a direct comparison of recurrence intervals with and without anthropogenic forcing is not possible. Examination of lower thresholds illustrates the difference in the DHM probability distributions with and without anthropogenic forcing. For example, the chance of DHM >0.5°C-month occurring in a given year is <2% without anthropogenic forcing but 28% with anthropogenic forcing (Table 1). This difference between the probability distributions suggests that the anthropogenic forcing over the 20th century has increased the likelihood of warm events like 2005 by an order of magnitude.

**Future Scenarios.** The projected occurrence of thermal stress for the 21st century for the 2005 bleaching region under “business-as-usual” conditions was obtained from simulations using SRES A1b (Fig. 7). Under this scenario, the mean annual SST is projected to increase by 2.2°C (CM2.0) and 2.3°C (CM2.1) from the 1990s to the 2090s. The projected increase in SSTs causes a sharp increase in the frequency of occurrences of severe thermal stress like 2005. Although the length of time required for a coral reef to recover from a mass coral bleaching event is highly variable, studies often assume that a recurrence interval of at least 5 years is required to ensure long-term maintenance of coral cover (5, 6). The models project that mean DHM would exceed 2°C-month at least biannually to annually ( $P = 60\text{--}80\%$ ) by the 2020s or 2030s (Fig. 7) and exceed the 2005 level in the HadISST data almost biannually by the 2030s ( $P = 40\%$ ).

In SRES B1, a lower emissions path over the century causes atmospheric CO<sub>2</sub> concentrations to stabilize at 550 ppm in the year 2100. The mean annual SST is projected to increase by 1.4°C (CM2.0) and 1.7°C (CM2.1) from the 1990s to the 2090s. Despite the lower increase in SSTs in this scenario, the projected increase in the occurrence of thermal stress is similar to that of the business-as-usual scenario (Fig. 7). The projected thermal stress on corals is similar in different future scenarios because of committed warming from past greenhouse gas emissions (6). By the time the climates in the two scenarios diverge in the middle of the century, the DHM >2°C-month threshold is being surpassed on a biannual basis. Under either scenario, the models project that thermal stress will exceed the 2005 level on an annual basis at the end of the century.

Recent evidence for flexibility in the coral–algal symbiosis and in the level of heterotrophic feeding by corals suggests the potential for coral reefs to adapt or acclimate to climate change (20–23). Some coral species have been observed to switch or shuffle symbionts in their tissues to more temperature-tolerant

*Symbiodinium* after bleaching events (20–22). For example, Berkelmans and Van Oppen (22) found that the common Indo-Pacific species *Acropora millepora* can increase its thermal tolerance level by 1–1.5°C by altering the dominant symbiont in its tissue from *Symbiodinium* clade C to the more temperature-tolerant clade D. Acquiring more temperature-tolerant *Symbiodinium* may come at a physiological cost and may not be possible for many corals (3, 22). Alternatively, a recent study suggests that some coral species could adapt after loss of symbionts, due to bleaching, by increasing their rate of heterotrophic feeding (23).

The theoretical impact of thermal acclimation or adaptation by Caribbean corals on the frequency of bleaching events was estimated by increasing the temperature at which thermal stress accumulates by 1°C and 1.5°C in the two scenarios (Fig. 7). In SRES A1b, adaptation of 1°C would delay the case of DHM >2°C-month occurring once every 5 years until the 2040s or 2050s, and the case of DHM > the 2005 level occurring once every 5 years until the 2050s or 2060s. Adaptation of 1.5°C would further delay the 5-year recurrence of severe bleaching until 2070s to the 2090s. This analysis suggests that, under business-as-usual conditions, overall thermal adaptation of 1–1.5°C could postpone (by ≈30–50 years or perhaps longer) mass coral bleaching from occurring at such a frequent interval that the corals are unlikely to recover. Such adaptation would, however, have implications for coral community structure, because the potential for increased thermal tolerance varies widely among coral species and growth forms (24, 25).

In SRES B1, adaptation of 1.5°C would prevent the harmfully frequent mass coral bleaching events from occurring this century. The annual DHM would not exceed 2°C-month more than once a decade at any point in the 21st century in the stabilization scenario (Fig. 7). However, climate models project long-term “committed warming” to occur after the stabilization of atmospheric CO<sub>2</sub> concentrations [e.g., figures 9.1 and 9.19 in Cubasch *et al.* (26)]. In the SRES B1 scenario, both CM2.0 and CM2.1 project a further 0.35°C in SSTs over the 22nd century, despite the stabilization of atmospheric CO<sub>2</sub> concentrations at 550 ppm in the year 2100. The models project that, with 1.5°C adaptation, mass coral bleaching may occur more than once every 5 years near the end of the 22nd century.

## Conclusions

This model-based assessment concludes that the observed warming trend in the region of the 2005 bleaching event is unlikely to be due to natural climate variability alone. Thermal stress of the level observed during the 2005 coral bleaching event is an exceedingly rare occurrence (>1,000-year event) absent the long-term warming trend. Under a business-as-usual scenario of future emissions, climate warming over the next 20–30 years could make thermal stress events like 2005 occur biannually. An increase in the magnitude, as well as the frequency, of thermal stress events could cause further coral mortality (27) and accelerate the reported decline of Caribbean coral reefs (28). A concurrent increase in Atlantic hurricane activity or intensity in the future, as suggested by several recent studies [refs. 7, 29, and 30; but see Landsea (31) for an alternative view], could potentially further damage coral reefs degraded by more frequent bleaching events.

Thermal adaptation by corals and their symbionts of 1.5°C could postpone the occurrence of frequent bleaching events that would threaten long-term coral cover in the Caribbean until the latter half of the century. Adaptation or acclimation to warmer temperatures might have some consequences for coral productivity and community structure (21, 24). The SRES B1 scenario, in which the atmospheric CO<sub>2</sub> concentrations are stabilized at twice the preindustrial level by the end of this century, suggests that thermal adaptation by corals may permit time to alter the

path of future greenhouse gas emissions and possibly prevent frequent and severe bleaching from becoming a regular occurrence in the latter half of the century. However, long-term committed warming projected after the stabilization of atmospheric greenhouse gas concentrations may represent a serious further threat to corals.

## Materials and Methods

The coupled models CM2.0 and CM2.1 have been used to conduct climate change simulations for the 2007 Intergovernmental Panel on Climate Change (IPCC) assessment. The models CM2.0 and CM2.1 are each composed of four component models: atmosphere, land, sea ice, and ocean. The key structural difference between the two models is the dynamical core in the atmospheric component. The climate sensitivities of CM2.0 and CM2.1 are 2.9°C and 3.4°C, respectively, in the middle range of models used in past IPCC assessments (e.g., table 9.1 in ref. 26).

The climate forcings used with these models to simulate past climate variations included well mixed greenhouse gases, ozone, anthropogenic tropospheric sulfates, black and organic carbon, volcanic aerosols, solar irradiance, and distribution of land cover types. Future projections used these same forcings, with the exception of no further volcanic emissions and no future changes in solar forcing or land cover. In using the model for assessment of historical climate variations and future projections, we assumed that the past and future forcings used are realistic, and that the models realistically represent the internal variability of the climate system and the response of the climate to the external forcings. We also assumed that the observed SST data sets accurately reflect true climate variations over the historical record. These two models are described in detail in Delworth *et*

*al.* (14), Knutson *et al.* (9), and references therein. Further information is available online at <http://nomads.gfdl.noaa.gov/CM2.X/references/>, and much of the model output data are freely available at <http://nomads.gfdl.noaa.gov/>.

The ocean component of CM2.0 and CM2.1 operates on a grid with longitudinal resolution of 1° and latitudinal resolution varying from 1° in the mid-latitudes to 1/3° at the equator. The latitudinal resolution becomes progressively fine from 30° (north and south) toward the equator; it varies from 0.67° to 0.88° in the study region. The satellite SST data set and HadISST data set were interpolated to this spatial grid to match the modeled SST output.

Throughout the study, we present the combination of model anomalies and observed climatology rather than direct model output, as is common in climate model studies. For example, the SST for January 1998 for a given simulation is estimated as the sum of the January SST in the observed climatology and the difference between the model value for January 1998 and the model climatology for January. We used the 1985–2000 satellite SST data as the observed climatology, to be consistent with the method of bleaching prediction. The model climatology for the 1985–2000 period was determined from the model ensemble results from the all-forcing simulations. Therefore, the annual simulated DHM for the year in any given simulation is the maximum accumulation of simulated SSTs (model anomaly plus satellite SST) in excess of the maximum monthly SST in the satellite climatology over a rolling 4-month period.

We thank Mark Eakin, William Skirving, and Scott Heron of the National Oceanic and Atmospheric Administration Coral Reef Watch for providing the satellite data and for helpful insight during this study. This research was made possible through the support of the High Meadows Leadership and Policy Fund.

1. Douglas AE (2003) *Mar Pollut Bull* 46:385–392.
2. Glynn PW (1991) *Trends Ecol Evol* 6:175–179.
3. Hoegh-Guldberg O (1999) *Mar Freshw Res* 50:839–866.
4. Wellington GM, Glynn PW, Strong AE, Navarette SA, Wieters E, Hubbard D (2001) *EOS, Trans Am Geophys Union* 82:1–6.
5. Sheppard CRC (2003) *Nature* 425:294–297.
6. Donner SD, Skirving WJ, Little CM, Oppenheimer M, Hoegh-Guldberg O (2005) *Glob Change Biol* 11:2251–2265.
7. Mann ME, Emanuel KA (2006) *EOS, Trans Am Geophys Union* 87:233–244.
8. Trenberth KE, Shea DJ (2006) *Geophys Res Lett* 33:L12704.
9. Knutson TR, Delworth TL, Dixon KW, Held IM, Lu J, Ramaswamy V, Schwarzkopf D, Stenchikov D, Stouffer RJ (2006) *J Clim* 19:1624–1651.
10. Santer BD, Wigley RML, Glecker PJ, Bonfils C, Wehner MF, AchutaRao K, Barnett TP, Boyle JS, Bruggemann W, Fiorino M, *et al.* (2006) *Proc Natl Acad Sci USA* 103:13905–13910.
11. Goldenberg SB, Landsea CW, Mesta-Núñez AM, Gray WM (2001) *Science* 293:474–479.
12. Liu G, Strong A, Skirving WM (2003) *EOS, Trans Am Geophys Union* 84:137–141.
13. Skirving WJ, Strong AE, Liu G, Arzayus F, Liu C, Sapper J, Bayler E (2006) in *Remote Sensing of Aquatic Coastal Ecosystem Processes*, eds Richardson LL, LeDrew EF (Springer, New York), pp 11–26.
14. Delworth TL, Broccoli AH, Rosati A, Stouffer A, Balaji V, Beesley JA, Cooke WF, Dixon KJ, Dunne J, Durachta JW, *et al.* (2006) *J Clim* 19:643–674.
15. Rayner N, Parker D, Horton E, Folland C, Alexander L, Rowell D, Kent E, Kaplan A (2003) *J Geophys Res* 108(D14):4407.
16. Barton AD, Casey KS (2005) *Coral Reefs* 24:536–554.
17. Schlesinger ME, Ramankutty N (1994) *Nature* 367:723–726.
18. Delworth TL, Mann ME (2000) *Clim Dyn* 16:661–676.
19. Stott PA, Stone DA, Allen MR (2004) *Nature* 432:610–614.
20. Baker AC, Starger CJ, McClanahan TR, Glynn PW (2004) *Nature* 430:741.
21. Little AF, van Oppen MJH, Willis BL (2004) *Science* 304:1492–1494.
22. Berkelmans R, van Oppen MJH (2006) *Proc R Soc London Ser B* 273:2305–2312.
23. Grotto AG, Rodrigues LJ, Palardy JE (2006) *Nature* 440:1186–1189.
24. Loya Y, Sakai K, Yamazato K, Nakano Y, Sambali H, van Woesik R (2001) *Ecol Lett* 4:122–131.
25. McClanahan TR (2004) *Mar Biol* 144:1239–1245.
26. Cubasch U, Meehl GA, Boer GJ, Stouffer RJ, Dix M, Noda A, Senior CA, Raper S, Yap KS (2001) in *Climate Change 2001: The Scientific Basis: Contribution of Working Group I*, eds Houghton JT, Ding Y, Griggs DJ, Noguer M, van der Linden PJ, Dai X, Maskell K (Cambridge Univ Press, New York), pp 525–582.
27. McWilliams JP, Cote IM, Gill JA, Sutherland WJ, Watkinson AR (2005) *Ecology* 86:2055–2060.
28. Gardner TA, Cote IM, Gill JA, Grant A, Watkinson AR (2003) *Science* 301:958–960.
29. Knutson TR, Tuleya RE (2004) *J Clim* 17:3477–3495.
30. Oouchi K, Yoshimura J, Yoshimura H, Mizuta R, Kusunoki S, Noda A (2005) *J Meteorol Soc Japan* 84:259–276.
31. Landsea CW (2005) *Nature* 438:E11–E12.